Parameterization and Validation of Solvation Corrected Atomic Radii†

Chun-Shan Zuo,[+,‡] Olaf Wiest,*[,§] and Yun-Dong Wu*[,+,‡,||]

Laboratory of Chemical Genomics, Shenzhen Graduate School of Peking University, Shenzhen, China, Department of Chemistry and Biochemistry, University of Notre Dame, Notre Dame, Indiana 46556-5670, State Laboratory of Molecular Science, College of Chemistry and Molecular Engineering, Peking University, 100871, Beijing, China, and Department of Chemistry, The Hong Kong University of Science and Technology, Clear Water Bay, Kowloon, Hong Kong, China

Received: June 22, 2009; Revised Manuscript Received: August 6, 2009

The use of correct ion radii is essential for the calculation of free energies of hydration using continuum models. A simple method for the fitting of the ion radii for ions in aqueous solution, which is a consistently difficult problem for implicit solvent models, is described. A new set of ionic radii based on experimental ionic hydration free energies for use in the integral equation formalism of polarizable continuum model (IEFPCM) is derived using B3LYP calculations with a 6-311++g** basis set for Li, Na, K, Be, Mg, and Ca and a SDD basis set for all other metals. The new radii reproduce the experimental stability constants of metal ions and their pyridine, 2,2′-bipyridine, and 1,10-phenanthroline complexes in aqueous solution significantly better than the results obtained using the default UAHF ion radii. The standard deviation (SD) of binding free energies between the calculations and experiments for the metal−ligand complexes in aqueous solution is 3.7 kcal/mol, while the mean unsigned error (MUE) is 3.1 kcal/mol. These results improve on the standard UFF radii for metal atoms, in which the MUE and the SD are 30.4 and 16.9 kcal/mol, respectively. The new ionic radii greatly improve the computational tools for the study of a variety of metals with ligands such as pyridines or calixarenes, which have found significant interest in materials science and for the removal of toxic metals.

Introduction

Solvent effects play important roles for molecular structures, energies, and properties since most of chemical processes occur in solution and many approaches have been developed to deal with them in the past several decades.[1] These approaches can be divided into two categories, explicit and implicit solvent models. Explicit solvent models have been widely used in force-field-based molecular simulations[2] where both the solvent, usually in form of a periodic boundary box filled with solvent molecules, and the solute are treated explicitly during the calculations. Explicit models are also applied to quantum mechanics calculations, but the systems are limited due to computational difficulties.[3] In contrast, implicit models treat solvation as the interaction of a solute of a certain size, shape, and charge distribution with a solvent continuum of a given dielectric constant and, more recently, polarizability.[4] Implicit methods are widely used in quantum chemistry due to the much more unfavorable scaling of these methods, which are not able to treat large numbers of solvent molecules explicitly. Implicit models have also been applied to the simulation of biomolecules in recent years.[5]

The implicit solvent models can be further subdivided into physics-based and fitted methods.[6] An example of the physics-based type is the integral equation formalism polarizable continuum model (IEFPCM) implicit solvent model developed by Tomasi[7] and co-workers and the closely related model by Chipman.[8] The series of semiempirical solvent models called SMx developed by Cramer and Truhlar, with SM8 being the latest version, are an example of the later where a number of parameters are fitted to reproduce the free energy of solvation of a wide range of neutral and ionic species.[9] For a wide variety of systems, including charged systems, these approaches provide results consistent with experimental data.[10] However, the treatment of metal cations using implicit solvent models remains challenging. Often, the solvation shell of the cation is modeled using explicit solvent molecules and the small solute−solvent clusters are embedded in an implicit model.[11] The size and structural features of the solute−solvent cluster are usually specific for a certain metal ion.[11g] Even for simple metal ions, one or more shells of solvent molecules are frequently necessary to calculate the free energies of hydration, greatly increasing the computational effort needed due to the large size of the system and the sampling necessary.

An alternative approach to the problem of free energy of solvation of metal ions that is proposed here combines some features of both models in that it uses the rigorously derived formalism of the IEFPCM that is usually applied with physics-based parameters such as the UAHF ion radii. A single parameter, termed the solvation corrected atomic radius (SCAR), is fitted to reproduce experimental solvation free energies. The advantage is that a simple procedure can provide a set of ionic radii that will allow the more accurate calculation of free energies of solvation of systems similar to the training set without additional computational cost compared to the standard methods. The disadvantage is that the quality of the extrapolation beyond the training set is unclear and likely to be less than the more general fitted methods such as SM8, which can be applied to many different solutes and solvents. We therefore focused

† Part of the "Walter Thiel Festschrift".

* Corresponding author: fax, (+) 00852-23587391; e-mail, chydwu@ust.hk.
[+] Shenzhen Graduate School of Peking University.
[‡] Peking University.
[§] University of Notre Dame.
[||] The Hong Kong University of Science and Technology.

10.1021/jp905865g CCC: $40.75
Published on Web 08/31/2009

on a common and important problem, the solvation free energies and the related complexation of mono- and multivalent metal ions in water, where the performance of many standard methods with default values is poor but where good experimental data are available. To maintain comparability to previous studies that showed good performace of the IEFPCM method for neutral molecules,[1,6,9] we used the standard UAHF values for all other atoms studied here.

The energetics of the transfer of a metal ion from the gas phase to bulk solution normally cannot be measured directly. However, the differences of Gibbs solvation free energies between two species are known for many cases. Therefore, the solvation free energy of metal ions is usually referenced to the absolute solvation free energy of the proton according to eq 1.

$$M^{n+} + nH^{+}_{(aq.)} \overset{\Delta G^{\circ}(conv.)}{\rightleftharpoons} M^{n+}_{(aq.)} + nH^{+} \qquad (1)$$

The solvation free energy of the proton can in turn be determined using molecular beam studies of clusters in the gas phase.[12] Using these results, Gibbs free energy of formation of hydrated proton can be expressed by the free energy of formation in the gas phase $\Delta_f G^{\circ}[H^{+}_g]$, and the absolute hydration free energy of proton $\Delta G_{aq}{}^{\circ}[H^{+}]$ as shown in eq 2. The free energy of solvation of a metal ion can then be expressed by eq 3, indicating the dependence on the solvation free energy of the proton.

$$\Delta_f G^{\circ}[H^{+}_{aq.}] = \Delta_f G^{\circ}[H^{+}_g] + \Delta G_{aq}{}^{\circ}[H^{+}] \qquad (2)$$

$$\begin{aligned}\Delta G_{aq}{}^{o,conv.}[M^{n+}] &= \Delta G_{aq}{}^{\circ}[M^{n+}] - n\Delta_f G^{\circ}[H^{+}_{aq}] \qquad (3)\\ &= \Delta G\circ_{aq}[M^{n+}] - n\{\Delta_f G^{\circ}[H^{+}_g] + \Delta G\circ_{aq}[H^{+}]\}\end{aligned}$$

Marcus' absolute hydration free energies of cations $\Delta G_{aq}{}^{\circ}[M^{n+}]$ (Table 1) referred to the absolute hydration free energies of proton $\Delta G_{aq}{}^{\circ}[H^{+}]$ (−251.1 kcal/mol).[13] Tissandier et al.[12] proposed that the absolute hydration free energy of proton should be −264.0 kcal/mol, and take the volume variation of the ion from the gas phase to solution, the value of $-RT\ln(RT/P^{\circ}) = -1.9$ kcal/mol should be included. Thus, the value of absolute hydration free energy of proton is −265.9 kcal/mol, a value that has been widely used in the more recent implicit solvent models.[1,6,9b,14] On the basis of this, the hydration free energies of metal ions are updated accordingly in Table 1 ($\Delta_h G_{upd}$).

The absolute free energies of hydration of ions are sensitive to the absolute free energy of hydration of the proton. However, many physical quantities are less sensitive or insensitive to the absolute free energies of hydration of the proton, such as the free energies of hydration of neutral species, formation constants of complexes, etc. Thus, the formation constants (independent to hydration free energies of single metal ions) of a metal−ligand system rather than a single ion species were chosen as the test cases for the solvation-corrected ionic radii. In this work, metal−pyridine (Py), 2,2′-bipyridine (BPy), and 1,10-phenanthroline (Phen) complexes were chosen. Pyridine is one of the most common and important moieties in molecules to form complexes with metal ions. Its derivatives are widely employed in analytical chemistry, supramolecular chemistry, catalysis, and biological studies.[15] There are numerous experimental studies on metal−pyridine complexes via spectrometric methods in the gas phase and solution.[16] Theoretical studies have also explored the intrinsic interactions and properties of these complexes in the gas phase.[17] However, these theoretical studies do not match the experimental results in solution. Thus in this work, we attempt to apply the SCARs for the investigation of formation constants of MPy, MBPy, and MPhen complexes as a test of the new ionic radii.

Computational Methodology

Since the free energies of hydration are sensitive to ionic radii in PCM model, it is possible to obtain different ionic hydration free energies via modifying the ionic radii. The updated hydration free energies of metal ions($\Delta_h G_{M'}$) shown in Table 1 were obtained using the Marcus hydration free energies, eq 1, and Tissandier's absolute hydration free energies of proton. The correction energy of −14.8 kcal/mol between the Marcus and Tissander free energy of the proton, multiplied by the charge state of the metal, was added to the relevant Marcus hydration free energies of univalent, divalent, and trivalent metal ions, respectively. As expected, the updated hydration free energies of monovalent ions are very close to those proposed by Truhlar and co-workers.[9b]

We then performed a series of IEFPCM calculations on various metal cations where the ionic radius was varied in steps of 0.02 Å. The free energies of solvation from the IEFPCM calculations as a function of the ion radius include both the electrostatic and the smaller but non-negligable nonelectrostatic terms within the framework outlined by Tomasi and Barone.[7] The difference between experimental and computed free energy of solvation was then plotted against the chosen ionic radius. If the difference fell below a threshold of 0.5 kcal/mol, the radius was assigned as the SCAR of the ion. Figure S1 in the Supporting Information shows the case of Be^{2+} as an illustrative example.

For metal−ligand complexes, all geometry optimizations, vibration frequency analyses, and single point calculations for the free energies of hydration were carried out using the B3LYP[18] hybrid functional with the SDD basis set[19] for all the transition metal ions (including heavy metal atoms such as Pb, Rb, Cs, Sr, Ba) and the 6-311++g** basis set for all nonmetal atoms as well as Li, Na, K, Be, Mg, Ca). Single point calculations at the same level with integral equation formation of polarizable continuum model (IEFPCM) were employed to estimate the free energies of hydration of all components in the two sides of the reactions. All calculations were carried out using the GAUSSIAN03 series of programs.[20]

Results and Discussion

1. Gibbs Free Energies of Hydration of Metal Ions and Metal Ionic Radii. The results obtained for 36 different metal ions studied here are summarized in Table 1. The data set includes different charge states of the metal ion, where appropriate. Furthermore, water is a borderline case between low- and high-field ligands, but the spin states of metal ions in hydration depend on their electronic energies in the gas phase. Most ions studied here are in high spin states in the gas phase (except for Pb^{II}), but the results for both high and low spin cases are shown in Table 1. Experimental free energies of hydration ($\Delta_h G_M$) and Marcus ionic radii (r_M) of metal ions were taken from ref 13, the UAHF radii (r_U, UFF atomic radii instead for metal elements) and relative free energies of hydration ($\Delta_h G_U$) using these default radii are obtained from GAUSSIAN03 program packages directly. For comparison purposes, several

TABLE 1: Ionic Radii (r_M) and Absolute Free Energies of Hydration (Δ_hG_M) Compiled by Marcus, Updated Free Energies of Hydration Based on Marcus' Data (Δ_hG_{upd}), Pauling Radii (r_P) and Shannon Radii (r_S), UAHF Radii (r_U) and Relative Hydration Free Energies (Δ_hG_U), Solvation Corrected Atomic Radii (r_{mod}) and Relative Hydration Free Energies (Δ_hG_{mod}) Based on Marcus Free Energies, Solvation Corrected Atomic Radii ($r_{mod'}$), and Relative Hydration Free Energies ($\Delta_hG_{mod'}$) Based on Δ_hG_{upd}

	exptl[a]						UAHF[e]		modified		modified (upd.)	
ion	r_M	Δ_hG_M	Δ_hG_{upd}	r_P[b]	r_S[c]	r_S[d]	r_U	Δ_hG_U	r_{mod}	Δ_hG_{mod}	$r_{mod'}$	$\Delta_hG_{mod'}$
H^+	0.30	−251.1	−266.0		−0.38[i]	−0.18[j]						
Li^+	0.69	−113.6	−128.5[f]	0.74	0.59	0.76	1.226	−108.7	1.168	−113.5	1.042	−128.3
Cu^I	0.96	−125.5	−140.5[f]	0.96	0.60	0.77	1.748	−73.9	1.154	−125.5	1.075	−141.2
Na^+	1.02	−87.3	−102.2[f]	0.95	0.99[g]	1.02	1.492	−89.3	1.494	−87.6	1.292	−103.4
					1.00							
Ag^I	1.15	−102.8	−117.8[f]	1.26	1.02(sq[h])	1.15	1.574	−84.6	1.358	−103.0	1.248	−118.4
K^+	1.38	−70.5	−85.5[f]	1.33	1.37[g]	1.38	1.906	−70.0	1.842	−70.3	1.575	−85.6
NH_4^+	1.48	−68.1	−83.1[f]				1.770	−80.5				
Rb^+	1.49	−65.8	−80.7[f]	1.48	−	1.52	2.057	−60.3	1.883	−65.5	1.617	−80.1
Tl^+	1.50	−71.7	−86.7[f]	1.40		1.50	2.174	−56.8	1.842	−71.8	1.632	−86.3
Cs^+	1.70	−59.8	−74.7[f]	1.69		1.67	2.259	−53.4	2.025	−59.7	1.733	−74.7
Au^I				1.37	−	1.37	1.647	−80.8			1.184	−142.2
Be^{2+}	0.40	−572.7	−602.6	0.31	0.27	0.45	1.373	−394.7	0.950	−572.3	0.902	−603.3
$Ni^{II(s1)}$							1.417	−383.3	1.165	−473.4	1.099	−506.5
					1.00							
$Ni^{II(s3)}$	0.69	−473.5	−503.3	0.72	0.49(sq)[g]	0.69	1.417	−382.8	1.165	−471.8	1.099	−504.4
Mg^{2+}	0.72	−437.6	−467.5	0.65	0.57	0.72	1.511	−357.8	1.238	−437.7	1.158	−468.3
Cu^{II}	0.73	−480.6	−510.5	0.70	0.57(sq)	0.73	1.748	−307.9	1.144	−480.6	1.084	−511.3
$Co^{II(s2)}$					0.38[g]	0.65	1.436	−377.9	1.200	−458.3	1.134	−489.1
$Co^{II(s4)}$	0.75	−457.9	−487.8	0.74	0.58	0.75	1.436	−377.9	1.200	−458.0	1.134	−488.7
Zn^{II}	0.75	−467.5	−497.3	0.74	0.60	0.74[g]	1.382	−392.9	1.169	−467.8	1.104	−498.3
$Fe^{II(s1)}$						0.61	1.456	−372.8	1.246	−440.7	1.175	−471.3
$Fe^{II(s3)}$							1.456	−372.7	1.246	−440.3	1.175	−470.8
$Fe^{II(s5)}$	0.78	−440.0	−469.8	0.76	0.63(sq)	0.78	1.456	−372.8	1.246	−440.2	1.175	−470.5
$Mn^{II(s2)}$					0.67	0.81	1.481	−366.9	1.302	−421.0	1.218	−453.9
$Mn^{II(s6)}$	0.83	−420.9	−450.7	0.80	0.66	0.83	1.481	−366.3	1.302	−419.4	1.218	−451.4
$Pd^{II(s1)}$							1.450	−378.3	1.234	−456.7	1.166	−492.4
$Pd^{II(s3)}$	0.86	−456.7	−486.6	0.86	0.64	0.86	1.450	−378.3	1.234	−453.2	1.166	−487.7
Cd^{II}	0.95	−419.7	−449.5	0.97	0.78	0.95	1.424	−382.5	1.306	−419.8	1.228	−450.6
Ca^{2+}	1.00	−359.9	−389.7	0.99	−	1.00	1.700	−316.9	1.500	−359.5	1.386	−390.7
Hg^{II}	1.02	−420.9	−450.7	1.10	0.96[g]	1.02[g]	1.353	−409.3	1.319	−420.7	1.247	−451.8
Sr^{2+}	1.13	−330.0	−359.8	1.13		1.18	1.821	−295.1	1.632	−329.6	1.500	−360.7
$Pb^{II(s1)}$	1.18	−340.7	−370.6	1.20	0.98[g]	1.19[g]	2.149	−248.1	1.590	−340.4	1.499	−371.6
$Pb^{II(s3)}$							2.149	−251.7	1.590	−339.5	1.499	−395.6
Ba^{2+}	1.36	−298.9	−328.8	1.35		1.35	1.852	−290.2	1.793	−298.6	1.641	−329.4
$Co^{III(s1)}$						0.55	1.436	−852.6	1.145	−1074.8	1.099	−1122.0
$Co^{III(s3)}$							1.436	−852.6	1.145	−1074.6	1.099	−1121.6
$Co^{III(s5)}$	0.61	−1074.8	−1119.6	0.63	−	0.61	1.436	−852.6	1.145	−1074.5	1.099	−1121.4
$Fe^{III(s2)}$						0.55	1.456	−840.9	1.204	−1020.8	1.153	−1067.8
$Fe^{III(s4)}$							1.456	−841.2	1.204	−1021.1	1.153	−1068.2
$Fe^{III(s6)}$	0.65	−1019.8	−1064.6	0.64	0.49	0.65	1.456	−840.7	1.204	−1019.7	1.153	−1066.3
MUE								90.5		9.1		0.8
SD								70.4		26.6		0.5

[a] r_M and Δ_hG_M values are taken from ref 13b. $\Delta_hG_{M'}$ values are derived from Δ_hG_M values with eq 1. [b] Six-coordinated Pauling radii, compare ref 21. [c] Four-coordinated (to be tetrahedron without special notification) Shannon radii and six-coordinated Shannon radii taken from ref 22. [d] Four-coordinated (to be tetrahedron without special notification) Shannon radii and six-coordinated Shannon radii taken from ref 22. [e] UFF radii instead for metal ions in Gaussion03; compare ref 23. [f] These values can be compared with those in ref 9b. [g] Taken from ref 24. [h] Square planar coordination. [i] Mono-coordinated. [j] Bi-coordinated.

widely used ionic or atomic radii, such as Pauling radii (r_P) and Shannon radii (r_S), are also included in Table 1. Pauling and Shannon radii are derived from X-ray single crystal structures, while UAHF radii for metal ions in the Gaussian03 program use the parameters of UFF radii, which are derived from van der Waals radii multiplied by a prefactor and are therefore identical for different oxidation states of the metals. The UAHF radii are relatively larger than the ones proposed by Pauling and Shannon, consistent with the fact that radii used in implicit solvent calculation are larger than the covalent radii due to the noncovalent character of solvent interactions. The SCARs (r_{mod}) and the free energies of hydration obtained in IEFPCM calculations using the SCARs (Δ_hG_{mod}) based on Marcus free energies are summarized. Finally, the SCARs (r_{mod}') derived using the hydration free energies ($\Delta_hG_{M'}$) updated according to the Tissander free energies of hydration for the proton are shown. The mean unsigned error (MUE) and standard deviation (SD) for the values computed using the UAHF and SCARs relative to the corrected Marcus free energy of solvation are also given.

Figure 1 summarizes the results for the radii shown in Table 1 by comparing the radii assigned by Marcus based on the free energies of solvation to the UAHF and modified ionic radii. As mentioned previously, the UAHF radii are consistently ~30% larger than the Marcus radii and the correlation coefficient is about 0.71, relatively low. Comparison with the SCARs shows a significantly better agreement. The SCARs are about 15% larger than the Marcus radii and the correlation coefficient

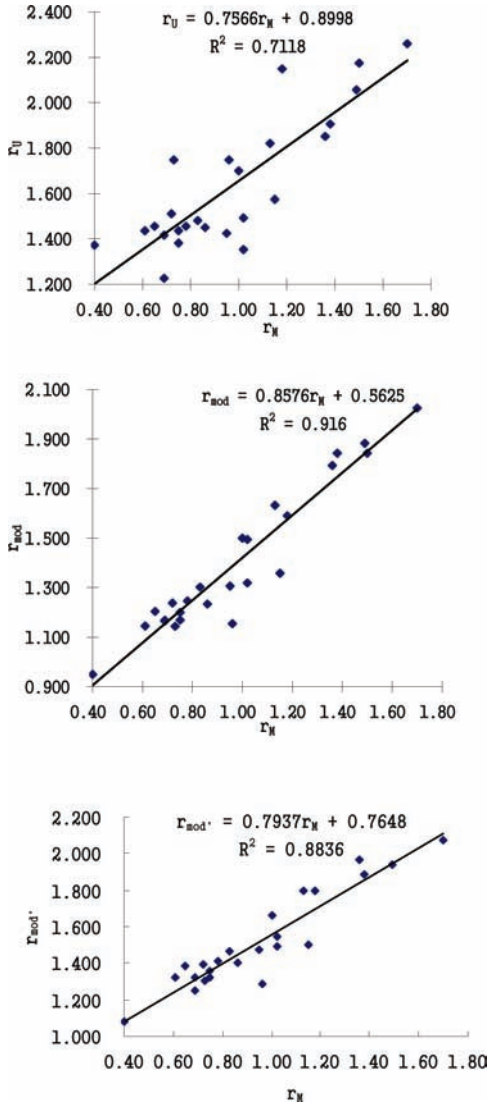

Figure 1. (a) Correlation between ionic radii by Marcus (r_M) (Å) and UAHF radii (r_U) (Å), (b) correlation between r_M and SCAR radii (r_{mod}) (Å), and (c) correlation between r_M and updated modified radii ($r_{mod'}$) (Å).

improves to 0.92. The slightly lower correlation coefficient between $r_{mod'}$ and r_M is most likely due to the uncertainty of hydration free energy correction for the higher charged cations, which leads to a much better correlation between the experimental and computational free energies of hydration.

The free energies of hydration obtained by using the UAHF radii in IEFPCM calculations consistently underestimate the free energies of hydration of metal ions comparing to Marcus' data, leading to a MUE of 86.7 kcal/mol with a standard deviation (SD) of 69.3 kcal/mol. More significantly, the experimental relative hydration free energies of univalent cations are in sequence of $Li^+ > Ag^I > Na^+ > Tl^+ > K^+ > NH_4^+ > Rb^+ > Cs^+$ while using UAHF radii, the sequence is $Li^+ > Na^+ > Ag^I > NH_4^+ > K^+ > Rb^+ > Tl^+ > Cs^+$. It is noteworthy that for nonmetal ions such as NH_4^+, the results from the UAHF radii agree much better with experimental data. The disagreement is even more pronounced for the di- and trications, as is to be expected for these highly charged species, with differences between experimental and computed values in excess of 200 kcal/mol. The linear regression shown in Figure 2 on the left indicates that this is again due to a consistent underestimation of the free energy of hydration as compared to the experimental

SCHEME 1: Thermochemical cycles

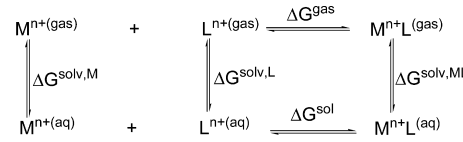

values. It is interesting to note that the coefficient of the linear regression is very similar to the one obtained from the correlation of the radii (Figure 1 top), but the R^2 value is with 0.977 much better.

The statistics for the free energy of hydration obtained with the modified ion radii in IEFPCM calculation are much improved. The MUE and standard deviation are now 27.0 and 9.1 kcal/mol, respectively. The linear regression shown in Figure 2 on the right has now an R^2 value of 0.9999 and a coefficient of 0.9689. These statistics and the essentially quantitative agreement (MUE and SD of 0.8 and 0.5 kcal/mol, respectively) with the free energies of hydration that were corrected for the new value for the free energy of hydration of the proton as discussed above demonstrate that the differences are almost entirely due to the chosen reference value. This indicates that the essential features of the solvation are well reproduced across the spectrum of mono-, di-, and trications for which comparison with experimental data is possible. An application to the study of metal complexes, where the free energy of complexation will significantly depend on the desolvation penalty of the ion in water, is therefore promising.

2. Gibbs Free Energies of Binding for Metal−Pyridine (MPy) and Metal−Bipyridine (MBPy) and Metal−Phenathroline (MPhen) Complexes. Pyridine can be considered as σ-electron donor and π-electron donor when binding to metal ions, but its σ-donor character is much stronger than its π-donor character.[16e] Thus, we will focus on the σ-complexes of a series of metal ions with pyridine, bipyridine, and phenanthroline complexes as depicted in Figure 3.

To evaluate the free energies of the binding processes, the free energies of solvation for the complex and its components as described by self-consistent reaction field (SCRF) calculations should be taken into consideration. The thermochemical cycles shown in Scheme 1 were employed.

The total reaction free energies can be decomposed into two parts, one is the free energies in the gas phase ($\Delta_r G^{gas}$) and the other is the sum of solvation free energies of all species ($\Sigma\Delta G^{solv,i}$) as shown in eq 4

$$\Delta_r G^{sol} = \Delta_r G^{gas} + \Sigma\Delta G^{solv.i} \quad (4)$$

Using these model systems, the SCARs were used to study the stability constants of a variety of metal−ligand complexes with pyridine, 2,2′-bipyridine, and 1,10-phenanthroline. Recently, these complexes have found considerable interest due to their materials and electronic properties,[24] as transition metal catalysts for a variety of reactions,[25] and for the complexation of metals by aza-calixarenes and other ligands.[26]

Figure 4 shows the structures of the silver complexes as representative examples and Table 2 summarizes the results for the metal−nitrogen bonds as well as the binding energies in the gas phase and in solution obtained using UAHF and r_{mod} ionic radii. Since there is repulsion between ortho-hydrogens on the two pyridyl groups, the bipyridine structures in complexes are twisted by 13.8°. Because there is only a single nitrogen donor in the metal−pyridine systems, the calculated bond

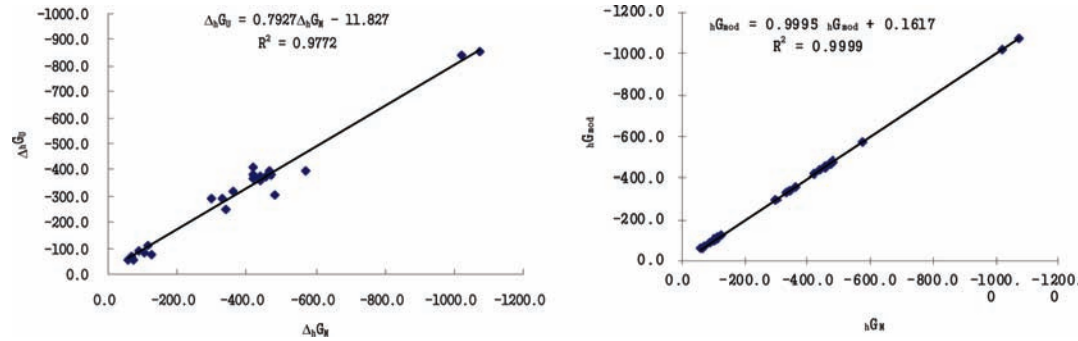

Figure 2. Correlation of the free energy of hydration as compiled by Marcus and the values obtained by IEFPCM calculations with UAHF (left) and that by SCARs (right).

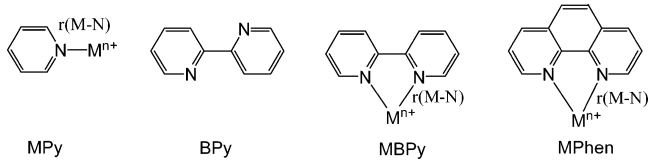

Figure 3. Geometry structures of MPy, BPy, MBPy, and MPhen.

lengths to the metal ions are consistently smaller than the ones in the corresponding bipyridine and phenanthroline ligands.

There are only very limited experimental gas phase data available that can be directly compared to the computed values. One of few cases is the bond dissociation energy for Ag^I-Py, which was determined by threshold collision-induced dissociation and photodissociation methods to be −45.2 kcal/mol.[16d] Subsequent theoretical studies computed values between −41.0 and −50.0 kcal/mol,[16d,j,17a] which are in line with the experimental results. Our result of −52.2 kcal/mol for the binding energy overestimates the experimental value by 7 kcal/mol. The metal−nitrogen distances in the two complexes are also slightly shorter than those calculated by Yang et al.[16d] and Wu et al.,[17a] indicating that gas phase binding interactions are slightly overestimated by our calculations.

The majority of binding studies of these complexes were conducted in solution The experimental stability constants in solution are in a range of $10^{0.7}-10^{8.7}$ for these complexes,[27] indicating Gibbs free energies ($\Delta_r G^{expt}$) for the formation of these complexes in the range of −1.0 to −12.0 kcal/mol. Comparison of the gas phase binding energies ΔE_b or free energies of binding $\Delta_r G^{gas}$ with the experimental binding energies in solution fails to correlate even qualitatively within a series. For example, Zn^{2+} is predicted to bind stronger to the BPy ligand but is in fact found experimentally to be a weaker binding metal. This is of course due to the different solvation contribution, re-emphasizing the need for an accurate description of solvation in for the accurate description of these complexes. Given the widespread interest in such metal−pyridyl complexes in organic and organometallic chemistry and the availability of experimental validation data, they are suitable test systems for the performance of the SCARs values in IEFPCM calculations.

We therefore compared the free energies of binding from IEFPCM calculations using standard UAHF radii (r_U) and SCARs (r_{mod}). The results are shown in Table 2 and Figure 5. It can be seen that the new ionic radii greatly improve the accuracy of the results. The mean unsigned error (MUE) is improved from 30.4 kcal/mol for UAHF radii to 3.1 kcal/mol for SCAR while the standard deviation drops from 16.9 to 3.7 kcal/mol. The linear regression, shown in Figure 5, indicates a correlation coefficient of $R^2 = 0.455$ for the results from the UAHF calculations. They also consistently overestimate the binding energy by a factor of almost 4 across the range of binding constants. In addition, the linear regression indicates a

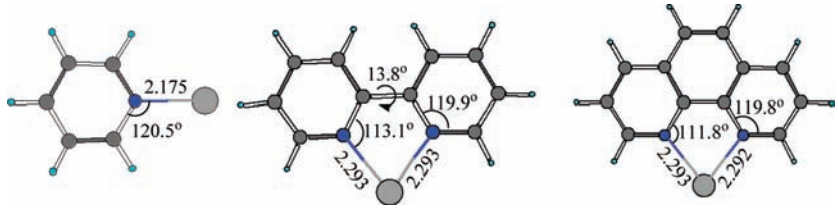

Figure 4. Structures of $[Ag-Py]^+$, $[Ag-BPy]^+$, and $[Ag-Phen]^+$

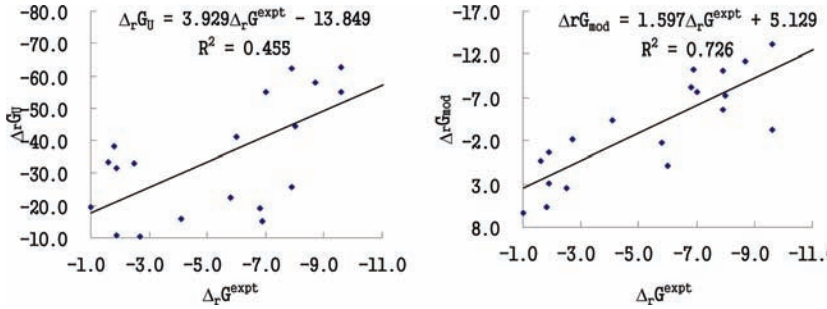

Figure 5. Correlation between calculated and experimental free energies of binding in solution obtained by the IEFPCM with UAHF (left) and SCAR (right) ion radii.

TABLE 2: Distance between the Metal Ions and Pyridine Nitrogen (r(M−N)) (Å), Binding Energies in the Gas Phase, and Interaction Energies (kcal/mol) in Solution with UAHF Radii (r_u) or SCAR Radii (r_{mod})

		gas phase			solution			
					UAHF radii		SCAR radii	
ligand	ion	Δ_rG^{expt} [a]	r(M−N)	Δ_rG^{gas} [d]	Δ_rG[c]	$\Delta\Delta_rG$	Δ_rG[d]	$\Delta\Delta_rG$
Py	Ag^{I}	−2.7	2.18	−44.5	−10.2	−7.5	−2.1	0.6
	$Fe^{II(s5)}$	−1.0	1.92	−146.1	−19.4	−18.5	6.4	7.4
	$Co^{II(s4)}$	−1.6	1.86	−170.4	−33.5	−31.9	0.3	1.8
	$Ni^{II(s3)}$	−2.5	1.89	−170.2	−33.2	−30.7	3.5	6.0
	Zn^{II}	−1.9	1.92	−174.4	−31.5	−29.5	−0.6	1.3
	Cd^{II}	−1.9	2.14	−139.6	−10.9	−8.9	2.9	4.8
	Hg^{II}	−6.9	2.15	−172.1	−15.1	−8.2	−10.3	−3.4
BPy	Ag^{I}	−4.1	2.29	−62.1	−16.0	−11.9	−4.4	−0.3
	$Fe^{II(s5)}$	−6.0	1.98	−223.9	−41.3	−35.2	0.9	6.9
	$Co^{II(s4)}$	−7.9	1.96	−247.9	−62.5	−54.6	−10.2	−2.3
	$Ni^{II(s3)}$	−9.6	1.91	−251.5	−55.0	−45.4	−3.3	6.2
	Zn^{II}	−7.0	1.94	−253.7	−55.0	−48.1	−7.6	−0.6
	Cd^{II}	−5.8	2.18	−202.0	−22.3	−16.6	−1.7	4.1
Phen	Ag^{I}	−6.8	2.29	−70.1	−19.3	−12.5	−8.2	−1.4
	Mg^{2+}	−1.8	2.01	−202.9	−38.2	−36.3	5.7	7.5
	$Fe^{II(s5)}$	−8.0	2.01	−229.2	−44.4	−36.5	−7.2	0.8
	$Co^{II(s4)}$	−9.6	1.96	−257.7	−62.9	−53.3	−13.1	−3.4
	$Ni^{II(s3)}$	−11.7	1.94	−265.6	−68.0	−56.3	−12.7	−1.0
	Zn^{II}	−8.7	1.95	−263.9	−57.9	−49.2	−11.2	−2.5
	Cd^{II}	−7.9	2.18	−212.5	−25.9	−18.0	−5.6	2.3
MUE						30.4		3.1
SD						16.9		3.7

[a] Reference 27. [b] Binding free energies of MPy, MBPy, and MPhen in the gas phase. [c] $\Delta_rG = \Delta_rG^{gas} + \Sigma\Delta_hG_i$ of eq 1, $\Delta\Delta_rG = \Delta_rG - \Delta_rG^{expt}$. [d] $\Delta_rG = \Delta_rG^{gas} + \Sigma\Delta_hG_i$ of eq 1, $\Delta\Delta_rG = \Delta_rG - \Delta_rG^{expt}$.

large intercept. Together, these findings indicate that the stabilization of the ions in solution is substantially underestimated.

In comparison, the modified ionic radii lead to a substantial improvement of the correlation coefficient to 0.726, together with a smaller coefficient of ∼1.6 and a smaller intercept. Taken together, these data show that the modified radii greatly improve the result of Gibbs free energies of formation of these metal−ligand complexes in water. The two biggest outliers are the Fe^{II}−BPy and Ni^{II}−BPy complexes, while the free energies of formation for the complexes of these metals with the other two ligands are reproduced well.

Conclusions and Outlook

The fitting of ion radii to the free energy of hydration within the IEFPCM model leads to a new set of parameters for a series cations that greatly improve on the accuracy and consistency of the calculated results compared to the standard UAHF values without added computational cost. Application to the binding free energies of metal−pyridine-type complexes demonstrate their utility in the study of a series of interesting compounds. These results are achieved by fitting a single parameter to the experimental free energy of solvation of the ions of interest.

The philosophy of this approach is quite different from the one followed in most other solvent models such as the SMx or COSMO models, where a significant number of parameters is fitted to a large and diverse data set to generate physically meaningful values that are general for different solvents and solutes. These parameters can then be applied not only for the calculation of free energies of binding but also potentially for a number of other molecular properties.[25]

The advantages of the method and ion radii presented here are that they can be generated efficiently and allow the fast and accurate calculation of free energies of solvation as well as the complexation of these ions by nitrogen-based ligands in aqueous solution. The disadvantage is that the values are not easily transferable to other solvents and cannot be estimated from other known quantities so that an explicit refitting will be necessary in these cases. In the present form, they allow for the study of the free energy of binding of the complexes of the parametrized metals with a range of organic ligands such as calixarenes. These studies are currently underway and will be reported in due course.

Acknowledgment. This research was supported by the National Science Foundation of China (20225312) and the Research Grants Council of Hong Kong (CA06/06.SC05).

Supporting Information Available: Cartesian coordinates, energies, and free energies in gas phase and in solution obtained with UAHF and modified ion radii. This material is available free of charge via the Internet at http://pubs.acs.org

References and Notes

(1) For recent reviews on the computation of solvation free energies calculations compare:(a) Cramer, C. J.; Truhlar, D. G. *Chem. Rev.* **1999**, *99*, 2161–2200. (b) Tomasi, J.; Mennucci, B.; Cammi, R. *Chem. Rev.* **2005**, *105*, 2999–3094. (c) Cramer, C. J.; Truhlar, D. G. *Acc. Chem. Res.* **2008**, *41*, 760–768. (d) Chipman, D. N. *Theor. Chem. Acc.* **2002**, *107*, 80–89.

(2) (a) Jorgensen, W. L.; Madura, J. D. *Mol. Phys.* **1985**, *56*, 1381. Berendsen, H. J. C.; Grigera, J. R.; Straatsza, T. P. *J. Phys. Chem.* **1987**, *91*, 6269–1987. (b) Mahoney, M. W.; Jorgensen, W. L. *J. Chem. Phys.* **2000**, *112*, 8910–8922.

(3) For examples of explicit water models in quantum mechanics studies see, e.g.::(a) Lee, H. M.; Tarakeshwar, P.; Park, J.; Kolaski, M. R.; Yoon, Y. J.; Yi, H.-B.; Kim, W. Y.; Kim, K. S. *J. Phys. Chem. A* **2004**, *108*, 2949–2958. (b) Hagberg, D.; Bednarz, E.; Edelstein, N. M.; Gagliardi, L. *J. Am. Chem. Soc.* **2007**, *129*, 14136–14137. (c) Zorn, D.; Lin, V. S. Y.; Pruski, M.; Gordon, M. S. *J. Phys. Chem. B* **2008**, *112*, 12753–12760.

(4) E.g.:(a) Marenich, A. V.; Olson, R. M.; Kelly, C. P.; Cramer, C. J.; Truhlar, D. G. *J. Chem. Theory Comput.* **2007**, *3*, 2011–2033. (b) Marenich, A. V.; Olson, R. M.; Chamberlin, A. C.; Cramer, C. J.; Truhlar, D. G. *J. Chem. Theory Comput.* **2007**, *3*, 2055–2067.

(5) (a) Bashford, D.; Case, D. A. *Annu. Rev. Phys. Chem.* **2000**, *51*, 129–152. (b) Chen, J. H.; Brook, C. L., III; Khandogin, J. *Curr. Opin. Struct. Biol.* **2008**, *18*, 140–148.

(6) For a concise discussion of the relationship between different implicit solvent models, see:(a) Klammt, A.; Mennucci, B.; Tomasi, J.; Barone, V.; Curutchet, C.; Orozco, M.; Luque, F. J. *Acc. Chem. Res.* **2009**, *42*, 489–492. (b) Cramer, C. J.; Truhlar, D. G. *Acc. Chem. Res.* **2009**, *42*, 493–497. (c) Ben-Amotz, D.; Underwood, R. *Acc. Chem. Res.* **2008**, *41*, 957–967. For a benchmark evaluation of various CPCM models see:(d) Takano, Y.; Houk, K. N. *J. Chem. Theor. Comput.* **2005**, *1*, 70–77.

(7) (a) Barone, V.; Cossi, M.; Tomasi, J. *J. Chem. Phys.* **1997**, *107*, 3210–3221. (b) Mennucci, B.; Tomasi, J. *J. Chem. Phys.* **1997**, *107*, 3032–3041. (c) Mennucci, B.; Tomasi, J. *J. Chem. Phys.* **1996**, *107*, 5151–5158. (d) Mennucci, B.; Cancès, E.; Tomasi, J. *J. Phys. Chem. B* **1997**, *101*, 10506–10517. (e) Tomasi, J.; Mennuncci, B.; Cancès, E. *J. Mol. Struct.* **1999**, *464*, 211–226. (f) Amovilli, C.; Barone, V.; Cammi, R.; Cance's, E.; Cossi, M.; Mennucci, B.; Pomelli, C. S.; Tomasi, J. *Adv. Quantum Chem.* **1999**, *32*, 227–261.

(8) (a) Chipman, D. M. *J. Chem. Phys.* **2006**, *124*, 224111. (b) Chipman, D. M.; Chen, F. W. *J. Chem. Phys.* **2006**, *124*, 144507. (c) Chipman, D. M. *J. Chem. Phys.* **2000**, *112*, 5558–5565.

(9) (a) Kelly, C. P.; Cramer, C. J.; Truhlar, D. G. *J. Phys. Chem. B* **2006**, *110*, 16066–16081. (b) Chamberlin, A. C.; Cramer, C. J.; Truhlar, D. G. *J. Phys. Chem. B* **2008**, *112*, 8651–8655. (c) Marenich, A. V.; Olson, R. M.; Chamberlin, A. C.; Cramer, C. J.; Truhlar, D. G. *J. Chem. Theory Comput.* **2007**, *3*, 2055–2067. (d) Marenich, A. V.; Olson, R. M.; Kelly, C. P.; Cramer, C. J.; Truhlar, D. G. *J. Chem. Theory Comput.* **2007**, *3*, 2011–2033. (e) Marenich, A. V.; Cramer, C. J.; Truhlar, D. G. *J. Chem. Theory Comput.* **2008**, *4*, 877–887.

(10) (a) Pliego, J. R., Jr.; Riveros, J. M *Chem. Phys. Lett.* **2002**, *355*, 543–546. (b) Fu, Y.; Liu, L.; Li, R.-Q.; Guo, Q. -X. *J. Am. Chem. Soc.* **2004**, *126*, 814–822. (c) Böes, E. S.; Livotto, P. R.; Stassen, H. *Chem. Phys.* **2006**, *331*, 142–158.

(11) (a) Tsushima, S.; Yang, T.; Mochizuki, Y.; Okamoto, Y. *Chem. Phys. Lett.* **2003**, *375*, 204–212. (b) Mochizuki, Y.; Tsushima, S. *Chem. Phys. Lett.* **2003**, *372*, 114–120. (c) Asthagiri, D.; Pratt, L. R.; Paulaitis, M. E.; Rempe, S. B. *J. Am. Chem. Soc.* **2004**, *126*, 1285–1289. (d) Uudsemma, M.; Tamm, T. *Chem. Phys. Lett.* **2004**, *400*, 54–58. (e) Rotzinger, F. P. *Chem. Rev.* **2005**, *105*, 2003–2038. (f) Bryantsev, V. S.; Diallo, M. S.; Goddard, W. A. *J. Phys. Chem. B* **2008**, *112*, 9709–9719. (g) Bryantsev, V. S.; Diallo, M. S.; van Duin, A. C. T.; Goddard, W. A. *J. Phys. Chem. B* **2009**, *113*, 9104–9112.

(12) Tissandier, M. D.; Cowen, K. A.; Feng, W.-Y.; Gundlach, E.; Cohen, M. H.; Earhart, A. D.; Coe, J. V. *J. Phys. Chem. A* **1998**, *107*, 7787–7794.

(13) (a) Marcus, Y. *Ion Solvation*; Wiley: Chichester, 1985; Chapter 5. (b) Marcus, Y. *J. Chem. Soc., Faraday Trans.* **1991**, *87*, 2995–2999.

(14) (a) Pliego, J. R.; Riveros, J. M. *Phys. Chem. Chem. Phys.* **2002**, *4*, 1622–1627. (b) Kelly, C. P.; Cramer, C. J.; Truhlar, D. G. *J. Phys. Chem. A* **2006**, *110*, 2493–2499. (c) Kelly, C. P.; Cramer, C. J.; Truhlar, D. G. *J. Phys. Chem. B* **2007**, *111*, 408–422.

(15) (a) Morris, D. E.; Ohsawa, Y.; Segers, D. P.; DeArmond, Keith M.; Hanck, K. W. *Inorg. Chem.* **1984**, *23*, 3010–3017. (b) Calabrese, J. C.; Tam, W. *Chem. Phys. Lett.* **1987**, *133*, 244–245. (c) Fochi, G.; Strahle, J.; Ginglt, F. *Inorg. Chem.* **1991**, *30*, 4669–4671. (d) Soldatov, D. V.; Dyadin, Y. A.; Lipkowski, J.; Suwinska, K. *Mendeleev Commun.* **1997**, 100–102. (e) von Zelewsky, A. *Coord. Chem. Rev.* **1999**, *190*, 811–825. (f) Ashenhurst, J.; Brancaleon, L.; Gao, S.; Liu, W.; Schmider, H.; Wang, S.; Wu, G.; Wu, Q. G. *Organometallics* **1998**, *17*, 5334–5341. (g) Ho, K. -Y.; Yu, W. -Y.; Cheung, K. -K.; Che, C. -M. *J. Chem. Soc., Dalton Trans.* **1999**, *158*, 1–1586. (h) Schubert, U. S; Eschbaumer, C. *Angew. Chem., Int. Ed.* **2002**, *41*, 2892–2926. (i) Schareina, T.; Kempe, R. *Angew. Chem., Int. Ed.* **2002**, *41*, 1521–1523. (j) Goher, M. A. S.; Escuer, A.; Mautner, F. A.; Al-Salem, N. *Polyhedron* **2002**, *21*, 1871–1876. (k) Du, M.; Guo, Y. _M.; Chen, S. -T.; Bu, X. -H.; Ribas, J. *Inorg. Chim. Acta* **2003**, *346*, 207–214. (l) Bakir, M.; Hassan, I.; Green, O. *J. Mol. Struct.* **2003**, *657*, 75–83. (m) Hamann, C.; Kern, J. -M.; Sauvage, J. -P. *Inorg. Chem.* **2003**, *42*, 1877–1883. (n) Tsukube, H.; Yamada, T.; Shinoda, S. *J. All. Comp.* **2004**, *374*, 40–45. (o) Shavaleev, N. M.; Barbieri, A.; Bell, Z. R.; Ward, M. D.; Barigelletti, F. *New J. Chem.* **2004**, *28*, 398–405. (p) Berry, J. F.; Cotton, F. A.; Lu, T. -B.; Murillo, C. A.; Roberts, B. K.; Wang, X. -P. *J. Am. Chem. Soc.* **2004**, *126*, 7082–7096. (q) Crowder, K. N.; Garcia, S. J.; Burr, R. L.; North, J. M.; Wilson, M. H.; Conley, B. L.; Fanwick, P. E.; White, P. S.; Sienerth, K. D.; Granger II, R. M. *Inorg. Chem.* **2004**, *43*, 72–78. (r) Zhang, F. -B.; Kirby, C. W.; Hairsine, D. W.; Jennings, M. C.; Puddephatt, R. J. *J. Am. Chem. Soc.* **2005**, *127*, 14196–14197. (s) Sarkar, S.; Sarkar, B.; Chanda, N.; Kar, S.; Mobin, S. M.; Fiedler, J.; Kaim, W.; Lahiri, G. K. *Inorg. Chem.* **2005**, *44*, 6092–6099. (t) Natrajan, L.; Burdet, F.; Pécaut, J.; Mazzanti, M. *J. Am. Chem. Soc.* **2006**, *128*, 7152–7153. (u) Gao, F.; Chao, H.; Zhou, F.; Xu, L. -C.; Zheng, K. -C.; Ji, L. -N. *Helv. Chim. Acta* **2007**, *90*, 205–215.

(16) (a) Wu, H. -F.; Brodbert, J. S. *Inorg. Chem.* **1995**, *34*, 615–621. (b) Ma, S. -G.; Wong, P.; Yang, S. S.; Graham Cooks, R. *J. Am. Chem. Soc.* **1996**, *118*, 6010–6019. (c) Kohler, M.; Leary, J. A. *J. Am. Soc. Mass Spectrom.* **1997**, *8*, 1124–1133. (d) Yang, Y. -S.; Hsu, W. -Y.; Lee, H. -F.; Huang, Y. -C.; Yeh, C. -S.; Hu, C. _H. *J. Phys. Chem. A* **1999**, *103*, 11287–11292. (e) Yang, Y. -S.; Yeh, C. -S. *Chem. Phys. Lett.* **1999**, *305*, 395–400. (f) Rodgers, M. T.; Stanley, J. R.; Amunugama, R. *J. Am. Chem. Soc.* **2000**, *122*, 10969–10978. (g) Amunugama, R.; Rodgers, M. T. *Int. J. Mass Spectrom.* **2000**, *195*−*196*, 439–457. (h) Hsu, H. -C.; Lin, F. -W.; Lai, C. -C.; Yeh, C. -S. *New J. Chem.* **2002**, *26*, 481–484. (i) Guo, W. -Y.; Liu, H. -C.; Yang, S. -H. *Int. J. Mass Spectrom.* **2003**, *226*, 291–304. (j) Rannulu, R. N.; Rodgers, M. T. *J. Phys. Chem. A* **2007**, *111*, 3465–3479.

(17) (a) Wu, D. -Y.; Ren, B.; Jiang, Y. -X.; Xu, X.; Tian, Z. -Q. *J. Phys. Chem. A* **2002**, *106*, 9042–9052. (b) Kaczorowska, M.; Harvey, J. N. *Phys. Chem. Chem. Phys.* **2002**, *4*, 5227–5233. (c) Wu, D. Y.; Hayashi, M.; Shiu, Y. J.; Liang, K. K.; Chang, C. H.; Yeh, Y. L.; Lin, S. H. *J. Phys. Chem. A* **2003**, *107*, 9658–9667.

(18) Becke's three hybrid exchange functional and Lee, Yang, Parr's correlation functional contained in GASSIAN03 program, refers to: (a) Becke, A. D. *J. Chem. Phys.* **1993**, *98*, 5648. (b) Lee, C.; Yang, W.; Parr, R. G. *Phys. Rev. B* **1988**, *37*, 785. (c) Miehlich, B.; Savin, A.; Stoll, H.; Preuss, H. *Chem. Phys. Lett.* **1989**, *157*, 200.

(19) Comparing to the relativistic all-electron approach, efficient core potential basis set SDD is suggested to be more efficient than other basis sets on metal−water systems, see: Gourlaouen, C.; Piquemal, J.-P.; Saue, T.; Parisel, O. *J. Comput. Chem.* **2005**, *27*, 142–156.

(20) Frisch, M. J. et al. *Gaussian03, Rev. C.02*; Gaussian, Inc.: Wallingford, CT, 2004.

(21) Marcus, Y. *Chem. Rev.* **1988**, *88*, 1475.

(22) Shannon, R. D. *Acta Crystallogr.* **1976**, *A32*, 751.

(23) Rappé, A. K.; Casewit, C. J.; Colwell, K. S.; Goddard, W. A., III; Skiff, W. M. *J. Am. Chem. Soc.* **1992**, *114*, 10024.

(24) (a) Braun-Sand, S. B.; Wiest, O. *J. Phys. Chem. A* **2003**, *107*, 285–291. (b) Braun-Sand, S. B.; Wiest, O. *J. Phys. Chem. B* **2003**, *107*, 9624–9628.

(25) (a) Carney, J. M.; Donoghue, P. J.; Wuest, W. M.; Wiest, O.; Helquist, P. *Org. Lett.* **2008**, *10*, 3903–3906. (b) Plummer, J. M.; Weitgenant, J. A.; Noll, B. C.; Lauher, J. W.; Wiest, O.; Helquist, P. *J. Org. Chem.* **2008**, *73*, 3911–3914.

(26) (a) Ma, M. L.; Wang, H. X.; Li, X. Y.; Liu, L. Q.; Jin, H. S.; Wen, K. *Tetrahedon* **2009**, *65*, 300–304. (b) Wang, M. X. *Chem. Commun.* **2008**, 4541–4551. (c) Kanbara, T. M.; Yamamoto, T. *Tetrahedron Lett.* **2002**, *43*, 7945–7948. (d) Gong, H. -Y.; Zhang, X. -H.; Wang, D. -X.; Ma, H. -W.; Zheng, Q. -Y.; Wang, M. -X. *Chem.*−*Eur. J.* **2006**, *12*, 9262–9275. (e) Gong, H. -Y.; Zheng, Q. -Y.; Zhang, X. -H.; Wang, D. -X.; Wang, M. -X. *Org. Lett.* **2006**, *8*, 4895–4898.

(27) (a) Martell, A. E.; Smithm, R. M. *Critical Stability Constants*; Plenum Press: New York, 1974. (b) Dean, J. A. *Lange's Handbook of Chemistry*; 15th ed.; McGaw Hill: New York, 1999; pp 8−99, (c) Kapinos, L. E.; Sigel, H. *Inorg. Chim. Acta* **2002**, *337*, 131–142.

JP905865G